Environmental Research 195 (2021) 110874

Contents lists available at ScienceDirect

Environmental Research

journal homepage: www.elsevier.com/locate/envres

The role of seasonality in the spread of COVID-19 pandemic

Xiaoyue Liu [a,b], Jianping Huang [a,b,*], Changyu Li [a,b], Yingjie Zhao [b], Danfeng Wang [b], Zhongwei Huang [a], Kehu Yang [c]

[a] College of Atmospheric Sciences, Lanzhou University, Lanzhou, China
[b] Collaborative Innovation Center for Western Ecological Safety, Lanzhou University, Lanzhou, China
[c] School of Basic Medical Sciences, Lanzhou University, Lanzhou, 730000, China

ARTICLE INFO

Keywords:
COVID-19
Seasonal cycle
Transmission pattern
Intervention strategies

ABSTRACT

It has been reported that the transmission of COVID-19 can be influenced by the variation of environmental factors due to the seasonal cycle. However, its underlying mechanism in the current and onward transmission pattern remains unclear owing to the limited data and difficulties in separating the impacts of social distancing. Understanding the role of seasonality in the spread of the COVID-19 pandemic is imperative in formulating public health interventions. Here, the seasonal signals of the COVID-19 time series are extracted using the EEMD method, and a modified Susceptible, Exposed, Infectious, Recovered (SEIR) model incorporated with seasonal factors is introduced to quantify its impact on the current COVID-19 pandemic. Seasonal signals decomposed via the EEMD method indicate that infectivity and mortality of SARS-CoV-2 are both higher in colder climates. The quantitative simulation shows that the cold season in the Southern Hemisphere countries caused a 59.71 ± 8.72% increase of the total infections, while the warm season in the Northern Hemisphere countries contributed to a 46.38 ± 29.10% reduction. COVID-19 seasonality is more pronounced at higher latitudes, where larger seasonal amplitudes of environmental indicators are observed. Seasonality alone is not sufficient to curb the virus transmission to an extent that intervention measures are no longer needed, but health care capacity should be scaled up in preparation for new surges in COVID-19 cases in the upcoming cold season. Our study highlights the necessity of considering seasonal factors when formulating intervention strategies.

1. Introduction

The COVID-19 pandemic continues to spread rapidly across the world, which poses a dire threat to international public health (Huang et al., 2020c; Kraemer et al., 2020; Lai et al., 2020; Li et al., 2020b). Despite the worldwide implementation of various intervention measures from national quarantines to school closures, the COVID-19 pandemic has resulted in huge disruptive impacts on almost the entire sectors of society (Chowdhury et al., 2020; Lian et al., 2020a) and overwhelmed the healthcare systems in many well-resourced countries (Kissler et al., 2020). Recently, multiple new, more transmissible variants of SARS-CoV-2 have been circulating globally (WHO, 2021). A first generation of COVID-19 vaccines has become available for general public since the end of 2020, while studies are still underway to test whether the vaccines are still effective against these new variants (Mahase, 2021). The world is entering a new phase in its fight against the COVID-19 pandemic, and how long will it take to embrace full resumption of pre-COVID-19 normalcy remains highly uncertain (Potvin, 2021).

The seasonal cycle is a ubiquitous feature of influenza and other respiratory viral infections, particularly in temperate climates (Martinez, 2018). Since the beginning of the outbreak, there was widespread speculation that COVID-19, like other respiratory viral infections, might exhibit some form of seasonality. Research has reported that the transmissibility of coronavirus can be affected by several meteorological factors, including temperature and humidity (Altamimi and Ahmed, 2020; Cai et al., 2007), which influences the survival of the virus in the transmission routes. Numerous epidemiological and laboratory studies have explored the relationship between COVID-19 transmission and meteorological factors, while these findings are controversial. Huang et al. (2020b) found that 60.0% of the confirmed cases of COVID-19 occurred in places where the air temperature ranging from 5 °C to 15 °C. A study by Sajadi et al. (2020) found that the substantial community outbreaks of COVID-19 are distributed in the regions with mean

* Corresponding author. College of Atmospheric Sciences, Lanzhou University, Lanzhou, China.
E-mail address: hjp@lzu.edu.cn (J. Huang).

https://doi.org/10.1016/j.envres.2021.110874
Received 16 October 2020; Received in revised form 19 January 2021; Accepted 8 February 2021
Available online 19 February 2021

temperatures between 5 and 11 °C, combined with low humidity (3–6 g/kg). However, Yao et al. (2020b) reported that no association between COVID-19 transmission and temperature in Chinese cities was found. A study has shown that the positive rate (26.9%) of exhaled breath from COVID-19 patients (Ma et al., 2020) is significantly higher than that of the surface (5.4%) and air (3.8%), indicating airborne transmission as the major transmission route (Wilson et al., 2020; Yao et al., 2020a; Zhang et al., 2020a). Since the virus can remain viable in the air for multiple hours under favorable conditions (van Doremalen et al., 2020), we can reasonably speculate that the virus can be affected by wind conditions such as wind speed and direction. A study has found that a low wind speed is significantly correlated with higher COVID-19 cases in Jakarta, Indonesia, and the highest COVID-19 cases in the area fit in with wind direction blows (Rendana, 2020). However, another case study in Turkey shows that COVID-19 spreads more in windy weather (Coşkun et al., 2021). Numerical simulation also indicates that the microdroplets can transport in the air farther than 10 feet (3.05 m) due to wind convection, causing a potential health risk to nearby people (Feng et al., 2020). Wind and air circulation, which both display seasonality, may also potentially influence the transmissibility of the virus.

In addition to the meteorological factors, environmental factors including air pollution are also found to be related to COVID-19 incidence (Coccia, 2020a, 2020b) and other respiratory infections (Tong, 2019). Exposure to fine particulate matter, O_3, and NO_2 can influence the immune system of the susceptible population (Glencross et al., 2020), which may exert a direct impact on the severity of COVID-19 symptoms and mortality. In United States, higher historical $PM_{2.5}$ exposures are found to be positively associated with higher county-level COVID-19 mortality rates after accounting for many area-level confounders (Wu et al., 2020). Bilal et al. (2020) found that $PM_{2.5}$, O_3, and NO_2 have a significant relationship with the outbreak of COVID-19 in Germany. Studies also show that the interactions between atmospheric stability (wind speed) and air pollution can affect the spread of COVID-19 cases. Low wind speed is unfavorable for horizontal dispersion of pollutants (Cai et al., 2017) and causes pollutants to be trapped near ground level. High concentration of air pollutants, associated with low wind speed may support longer permanence of viral particles in the polluted air, thus promoting the pollution-to-human transmission (Coccia, 2020c, 2020d).

Laboratory studies of SARS-CoV-2, the virus that causes the COVID-19, also pointed out that the stability of the virus in the air or on surfaces is sensitive to environmental conditions, including humidity, temperature, sunlight, etc. The virus is more stable at low-temperature and low-humidity conditions, whereas warmer temperature and higher humidity shorten half-life (Matson et al., 2020). SARS-CoV-2 can persist for 14, 7, and 1 day under laboratory conditions at 4 °C, 22 °C, and 37 °C, respectively. When the temperature is increased to 56 °C, the persistence is dramatically reduced to 10 min (Chin et al., 2020). Experiments have shown that SARS-CoV-2 can remain viable and infectious in aerosols for hours at room temperature (21 °C–23 °C) and a fixed relative humidity of 65% (van Doremalen et al., 2020). Another study shows that simulated sunlight can rapidly inactivate SARS-CoV-2 suspended in either simulated saliva or culture media and dried on stainless steel coupons (Ratnesar-Shumate et al., 2020).

Despite the strong sensitivity of SARS-CoV-2 to environmental conditions in labs, these studies fail to prove the direct meteorological influence under real-world conditions. Furthermore, the existing studies concerning the role of meteorological factors on the COVID-19 transmission dynamics under realistic conditions are mostly based on linear and non-linear statistical analysis (Prata et al., 2020; Xie and Zhu, 2020). Limitations in COVID-19 data availability and quality remain obstacles to conducting conclusive studies on this topic. The public health interventions taken by various countries may have complicated the association between meteorological factors and virus transmission (Audi et al., 2020). Compared with the statistical models, epidemiological models could serve to reveal the intrinsic impact of

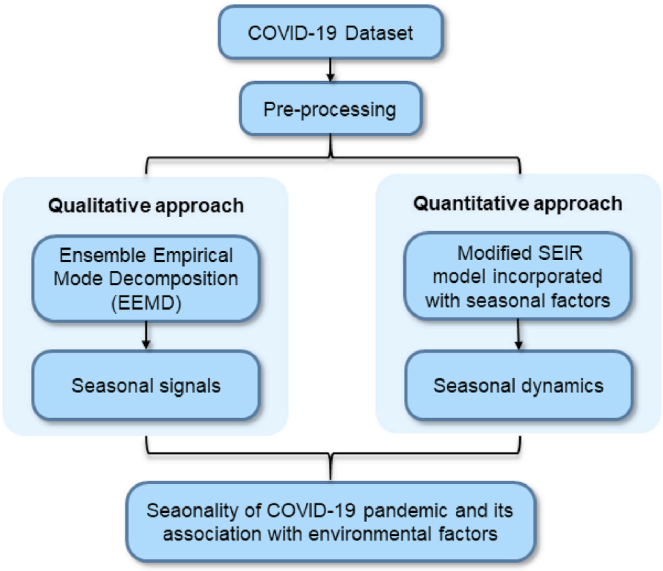

Fig. 1. Schematic illustration of assessing the influence of seasonality on COVID-19 pandemic.

under-reported cases and the intervention measures during the entire procedure of the outbreak (Harko et al., 2014; Peng et al., 2020), and have been widely used to examine the effects of non-pharmacological interventions around the world (Davies et al., 2020; Lai et al., 2020). In this study, the influence of seasonality on the spread of COVID-19 transmission is investigated both qualitatively and quantitatively (see Fig. 1). We first use an adaptive time-space analysis method (Ensemble Empirical Mode Decomposition, EEMD) to detect the seasonal signals in the time series of COVID-19 cases. Another approach, a modified version of the Susceptible, Exposed, Infectious, Recovered (SEIR) model incorporated with seasonality, is introduced to quantitatively explore the potential contribution of the seasonal cycle to the spread of the COVID-19 epidemic. The seasonal signals derived from the empirical (EEMD method) and process-based (compartmental model) models are analyzed and compared with seasonal signals of the meteorological and environmental factors. Finally, we propose a set of mechanisms through which the seasonal cycle of meteorological and environmental influence the transmission of COVID-19.

2. Data and method

2.1. Data source and country selection

The COVID-19 dataset (confirmed, recovered, and death cases) are collected from the COVID-19 Data Repository by the Center for Systems Science and Engineering (CSSE) at Johns Hopkins University (Dong et al., 2020). The dataset illustrates the location and number of confirmed COVID-19 cases, deaths, and recoveries for all affected countries in real-time. The data could be accessed through a Github repository (https://github.com/CSSEGISandData/COVID-19).

We will also analyze the correlation between environmental variables (meteorological factors and air quality) and the seasonality of COVID-19. For meteorological factors, we use near surface temperature and specific humidity of NCEP/NCAR reanalysis data (Kalnay et al., 1996). The NCEP/NCAR Reanalysis 1 project uses a state-of-the-art analysis/forecast system to perform data assimilation using past data from 1948 to the present. In this work, a climatology of 1980–2010 monthly means is calculated to present a seasonal cycle. Air quality data (total column NO_2 and $PM_{2.5}$ concentrations) are obtained from the EAC4 (ECMWF Atmospheric Composition Reanalysis 4). Observations from across the world are incorporated into a globally complete and

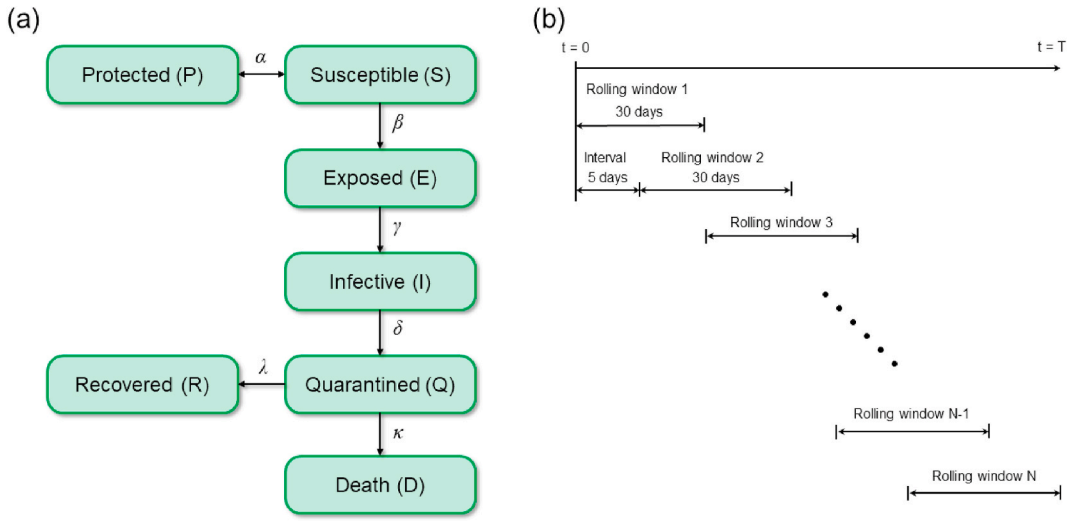

Fig. 2. The modified SEIR model (a) and rolling window method (b).

consistent dataset using a model of the atmosphere based on the laws of physics and chemistry. The observing system has changed drastically over time. Although the assimilation system can resolve data holes, the initially much sparser networks will lead to less accurate estimates. For this reason, EAC4 is only available from 2003 onwards. We calculated the climatology of 2003–2019 monthly mean to present the seasonal cycle.

The selection of countries is based on the following considerations. First, the seasonal cycle would exert a long-term effect on the development of the epidemic, and the effect may vary spatially and temporally. Second, the Northern Hemisphere (NH) and Southern Hemisphere (SH) experience opposite seasons. Thus, in order to identify and extract the long-term impact of seasonality from the pandemic data and reflect its spatial discrepancy, we select 5 countries in the NH and 5 countries in the SH. Fig. S1 shows the top 5 countries with the most confirmed cases in both NH and SH as of Dec 31st, 2020 (tropical countries that lie along the equator are excluded since the climate tends to be relatively even year-round). These countries (United States, India, Russia, France, United Kingdom, Brazil, Argentina, South Africa, Peru, and Chile) are 10 of the most affected regions by the COVID-19 pandemic, and contributed to 60.56% of the global cases as of Dec 31st, 2020. A wealth of outbreak data across different seasons in diverse climate zones makes it possible to draw out seasonal factors from the transmission dynamics.

2.2. EEMD method

We use the Ensemble Empirical Mode Decomposition (EEMD) method to detect the seasonal signals in the time series of COVID-19 confirmed cases in these countries. EEMD is an adaptive one-dimensional time series analysis method (Huang and Wu, 2008; Wu et al., 2007), which separates scales naturally without any prior subjective criterion. EEMD performs operations that partition a series into different 'modes' (Intrinsic Mode Functions, IMFs). The modes can provide insight into various signals contained within the data. This method has been widely applied in climatic and oceanic analysis (Ji et al., 2014), biomedical signal processing (Colominas et al., 2014), etc.

EEMD is a noise-assisted technique, and is meant to be more robust than simple Empirical Mode Decomposition (EMD). EEMD creates an ensemble of workers, each of which performs an EMD on a copy of the input signal with added noise. When all workers finish their work, a mean over all workers is considered as the true decomposition, and the noise will cancel each other out. In this study, the white noise added to data has an amplitude that was 0.05 times the standard deviation of the raw data, and the ensemble number is 100. The result of EEMD could be expressed by the following equation:

$$X(t) = \sum_{i=1}^{n} IMF_i(t) + r_n(t), \tag{1}$$

where $IMF_i(t)$ is the ith IMF, and $r_n(t)$ is the residual of data $X(t)$, which is monotonic or containing only one extremum from which no additional oscillatory components can be extracted. As demonstrated in previous studies (Ji et al., 2014; Wu et al., 2007), the extracted trend (r_n) follows no priori, and also has low sensitivity to the extension (addition) of new data. This property guarantees that the physical interpretation within specified time intervals does not change with the addition of new data, consistent with a physical constraint that the subsequent evolution of a system cannot alter the reality that has already happened.

A python module (PyEMD) for EEMD is available at https://www.github.com/laszukdawid/PyEMD (Laszuk, 2017). Since the prevalence of COVID-19 varies significantly across countries, for comparison we scale the time series of each country so that they range between 0 and 1 before conducting EEMD.

2.3. The modified SEIR model and parameter estimation

The SEIR model defines the four stages: the susceptible (S), exposed (E), infective (I), and recovered (R). However, the SEIR model may be oversimplified to simulate and predict the ongoing COVID-19 pandemic. Presymptomatic and asymptomatic transmission have been reported to play significant roles (Oran and Topol, 2020). Additionally, to contain the outbreak, a package of unprecedented social distancing measures has been implemented worldwide. Thus, a lot of variants of the SEIR model have been developed (Huang et al., 2020a). In this paper, we employed one of the modified versions (Cheynet, 2020; Peng et al., 2020). The model (see Fig. 2a) consists of the following equations:

$$\frac{dS(t)}{dt} = -\frac{\beta I(t) S(t)}{N} - \alpha S(t) \tag{2}$$

$$\frac{dP(t)}{dt} = \alpha S(t) \tag{3}$$

$$\frac{dE(t)}{dt} = \frac{\beta I(t) S(t)}{N} - \gamma E(t) \tag{4}$$

$$\frac{dI(t)}{dt} = \gamma E(t) - \delta I(t) \tag{5}$$

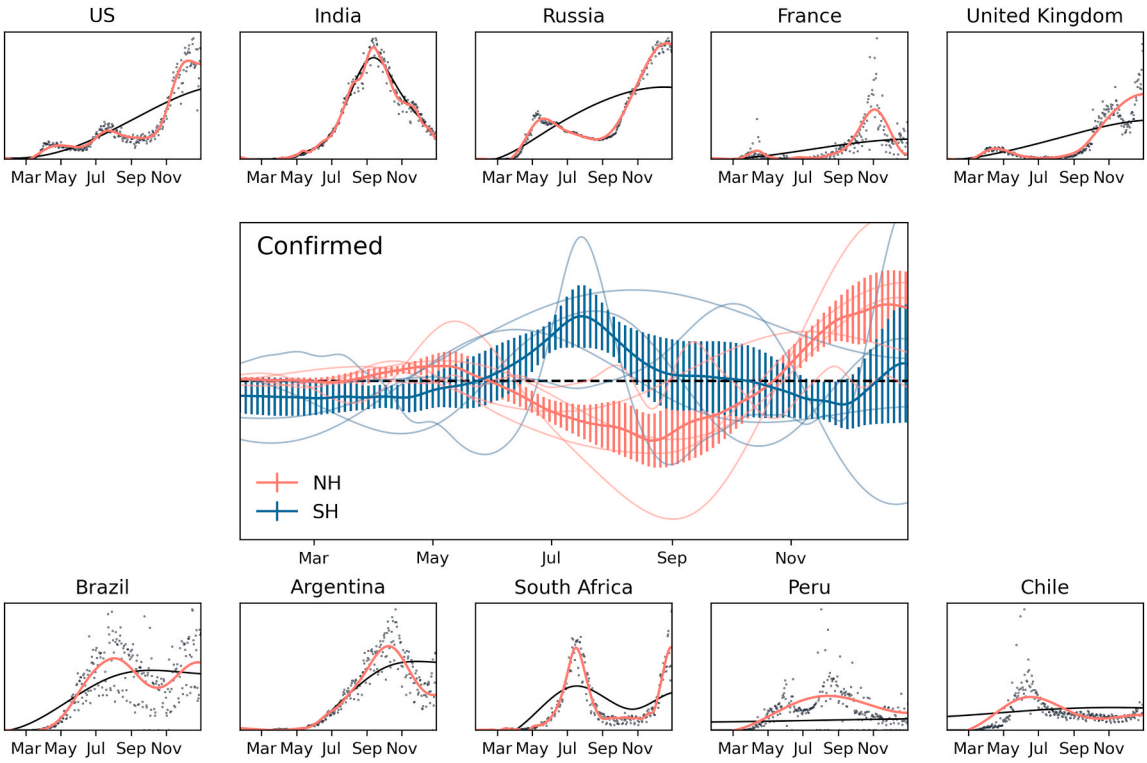

Fig. 3. Seasonal signals of confirmed cases in the five NH and five SH countries decomposed by the EEMD method. The top and bottom panels show the overall trend (black curves) and the trend superimposed with seasonal oscillation (red curves). The middle panel shows the seasonal oscillations for the selected NH (red) and SH (blue) countries. The red and blue thick curves denote the average seasonal signals for NH and SH, respectively, with error bars indicating 95% confidence intervals.

$$\frac{dQ(t)}{dt} = \delta I(t) - \lambda Q(t) - \kappa Q(t) \tag{6}$$

$$\frac{dR(t)}{dt} = \lambda Q(t) \tag{7}$$

$$\frac{dD(t)}{dt} = \kappa Q\ (t) \tag{8}$$

This version of the SEIR model adds several new groups of population: the protected (P), the quarantined (Q), and separates the recovered (R) and dead (D) cases. In this model, the susceptible (S) can either be protected to become the protected (P) at the rate of α (protection rate) or get infected to become the exposed (E) at the rate of β (transmission rate). After an individual is infected, it will take a certain period of time (pre-infectious period, $1/\gamma$) before he or she becomes infectious (I, capable of transmitting the virus to susceptible individuals). The infectious will then spread the virus to others before admitted to the hospital at the rate of δ (entering the quarantined stage, Q). The quarantined people cannot spread the virus and will be reported either as the recovered cases (R) or, unfortunately, death cases (D). λ and κ are the recovery rate and death rate, respectively. The parameters describing the transition between the stages (except α) are all positive numbers. When $\alpha>0$, individuals are passed from group S to group P, indicating the implementation of social distancing measures. When $\alpha<0$, individuals would return from group P to group S, demonstrating the relaxation of restrictions. The parameters in this model (α, β_0, β_1, γ, λ, δ, and κ) determines the rate of transition between stages (S, P, E, I, Q, R, and D), and shapes the epidemic curves. It should be noted that the infectious population is defined as the population capable of transmitting the virus, including the symptomatic, asymptomatic, and presymptomatic. We do not separate the asymptomatic, and presymptomatic from the infectious group due to the high uncertainty of the reported proportions of presymptomatic and asymptomatic transmission (Yanes-Lane et al., 2020). Adding additional unknown stages would make the model harder to constrain and significantly undermine the model stability, since only the data of three stages (Q, R, and D) are available to constrain the model parameters. The retrieved transmission rate (β) reflects the average transmissibility of COVID-19 in different transmission paths. This work aims to quantify the overall effect of seasonality on the COVID-19 transmission pattern.

We further modified the model by incorporating the seasonality factor in the transmission rate (β). Currently, 4 known seasonal coronaviruses circulate in human populations, including 2 alpha-coronaviruses (NL63 and 229E) and 2 beta-coronaviruses (OC43 and HKU1) (Kissler et al., 2020; Li et al., 2020a). Like seasonal influenza, they are more prevalent in the winter months. SARS-CoV-2 is one of the beta-coronaviruses and it is reasonable to speculate that SARS-CoV-2 would follow a similar seasonal pattern. Thus, we define β as a function of seasonality:

$$\beta(t) = \beta_0(t)[1 + \beta_1(\mathrm{t})\cos(\frac{2\pi t}{365} + \phi)]. \tag{9}$$

β_0 is the non-seasonality transmission rate, which is associated with the virus itself, population density, etc. β_1 is the amplitude of seasonal forcing, which modulates the transmissibility throughout the year. t denotes the day of the year. ϕ is set to 0 (π) in the NH (SH) to describe the anti-phases in the opposite hemispheres. The theoretical time curve of $\beta(t)$ for both NH and SH is shown in Fig. S2.

However, it should be noted that Eq. (9) is not undisputed. In some regions of the world, the transmission capacity of SARS-CoV-2 is not significantly reduced during the summer seasons, and the underlying mechanisms remain unclear (Carlson et al., 2020). Therefore, Eq. (9) could be replaced with other functions obtained in future epidemiological and laboratory studies concerning the environmental sensitivities of SARS-CoV-2.

The parameters (α, β_0, β_1, γ, λ, δ, and κ) are optimized using the nonlinear least-squares algorithm (Levenberg-Marquardt method). The algorithm finds the model parameters that minimize the sum of the

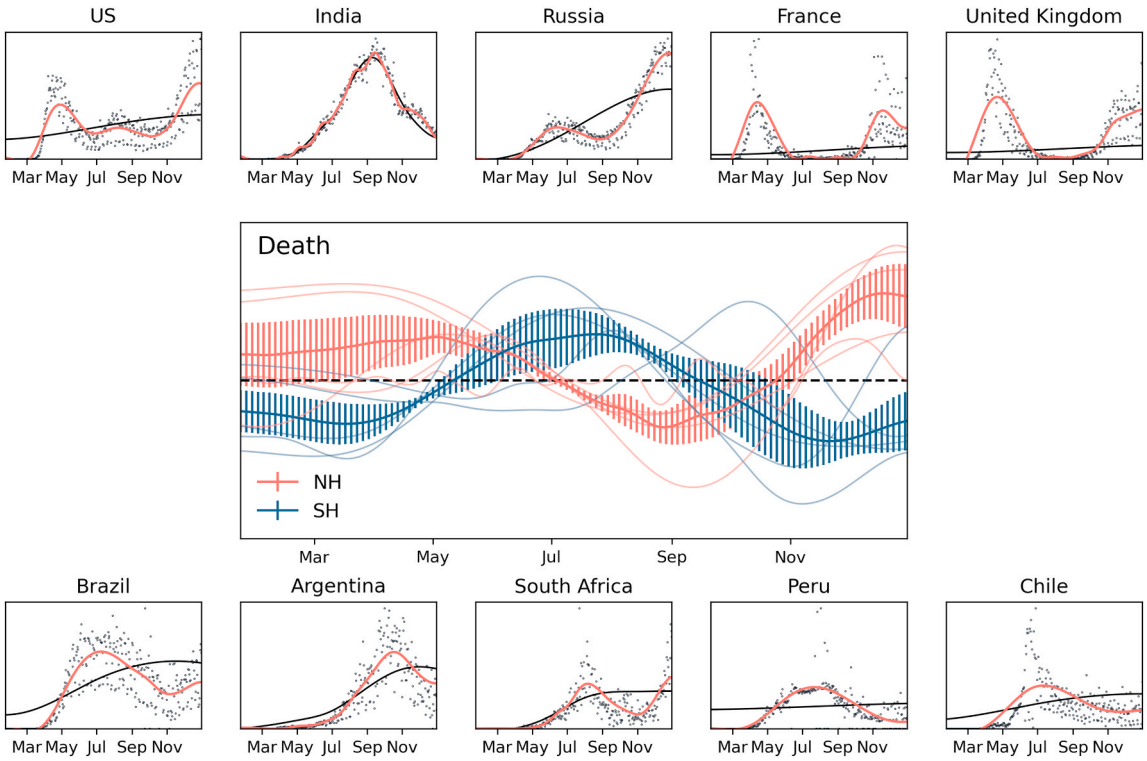

Fig. 4. Same as Fig. 3, but for death cases.

squared point-by-point distances between the model prediction and the data (residual). The values of parameters (α, β_0, β_1, γ, λ, δ, and κ) are determined when the residual reaches its minimum. To define a realistic range of these parameters and understand their meaning, the upper and lower boundaries of the parameters are set (See Table S1).

Since the local authorities would adjust the intervention strategy in different phases of the outbreaks, the parameters in the model should variate accordingly. In addition, the parameters describing the transmission capacity (β_0 and β_1) are not biological constant, and would also be affected by environmental conditions and behaviors of the infected individuals. Therefore, a rolling window method is employed to retrieve the parameters on a regular basis (window size = 30 days, interval = 5 days, see Fig. 2b). The differential equations are numerically solved by the 4th order Runge–Kutta method. In the simulation of the scenarios without seasonality, β_1 is set to zero to exclude the contribution of the seasonal cycle to the transmission rate $\beta(t)$.

The reported data in the selected countries are preprocessed before they are introduced to fit the parameters. In the initial stage of the outbreak, the quality of the reported data might be influenced by the lack of local medical capacity. The introduction of these early-stage data could result in large uncertainty of the model simulation. Therefore, we set an empirical threshold to introduce the reported data into our model when the local confirmed cases reach 1000. The time range of the data introduced in the simulation for each country is listed in Table S2.

3. Result

3.1. Seasonal signals in the COVID-19 time series

To extract the seasonal oscillation of the COVID-19 time-series, we decomposed the time series of daily confirmed and death cases of the ten countries from both NH and SH. Before the decomposition, the COVID-19 time series of each country are scaled so that their values range between 0–1, which makes it possible to compare the amplitude and phase of the intrinsic oscillation of different countries. The full decomposition result, as shown in Figs. S3–S12, can reveal the oscillation characteristic of the COVID-19 time series in different timescales (weekly, subseasonal, and seasonal). In weekly oscillations of the selected countries, high values usually occur during the weekdays and low values during the weekend. This is associated with high testing capacity and relatively short reporting delay during the weekday and low testing capacity and long reporting delay during the weekend (Dehning et al., 2020). For some countries (US, France, United Kingdom, and Brazil), the scaled confirmed and death cases indicate that the death rate of the resurgence during wintertime is significantly lower than the first surge, which might be associated with expanded medical resources.

For seasonal oscillation, the NH and SH are almost in the opposite phase, as shown in Figs. 3 and 4. In SH countries, the seasonal signals for confirmed and death cases peak on Jul. 16th and Jul. 24th, which is the coldest time of the year. For NH countries, however, the signals reach the trough during the warmest time of the year, on Aug. 22nd for confirmed cases and Aug. 28nd for death cases. The seasonal signals in NH countries show a significant upward trend as winter comes. The zero-crossing point of the seasonal signals could be interpreted as the seasonal transition point. In SH countries, the cold phase is between May 23rd and Oct. 10th for confirmed cases, and between May 11th and Sep. 15th. For NH, the warm phase for confirmed (death) cases is between May 30th and Oct. 22nd (Jul. 3rd and Oct. 24th). The zero-crossing points for both NH and SH are generally consistent with the seasonal cycle of meteorological variables.

Overall, the seasonal signals decomposed via the EEMD method indicate that infectivity and mortality of SARS-CoV-2 are both stronger in colder climates. However, it should be noted that the signals are also influenced by the effect of non-pharmacological interventions, including lockdowns, mandated face covering, etc. The EEMD signals can only provide a qualitative estimation of the seasonal impact. In the following section, we will employ a process-based model to simulate the COVID-19 curves so that a quantitative result could be offered.

3.2. Simulation of COVID-19 pandemic using modified SEIR model

Here, we use a modified SEIR model (See section 2) to simulate the

Table 1
Validation of the modified SEIR model. The numbers in the brackets denote the 95% confidence intervals.

	R_{total}	R_{daily}
NH countries	0.9997 (0.0007)	0.9772 (0.0448)
SH countries	0.9999 (0.0001)	0.9153 (0.1017)

evolution of the COVID-19 pandemic in the selected countries, and quantify the impact of seasonality on it. We first use the COVID-19 dataset to fit the model parameters with a rolling window method (See Fig. 2b). Then, we solve the modified SEIR model using the fitted parameters (α, β_0, β_1, γ, λ, δ, and κ). The solutions of the SEIR model are validated against the observation (reported COVID-19 dataset). Figs. S13 and S14 show the correlation between the simulated and reported cases in the 10 countries, with Pearson correlation coefficients at the upper-left corner of the sub-figures. R_{daily} refers to the correlation coefficients between simulated and reported daily increments, while R_{total} refers to the correlation coefficients between simulated and reported accumulated cases. The SEIR model proposed in this study faithfully reproduced the outbreak development, with averaged R_{total} (R_{daily}) reaching 0.999 (0.90) (see Table 1).

In our model, the seasonality of transmission rate is reflected in β_1 in Eq. (9). Thus, the transmission rate without seasonality can be obtained by setting the term containing β_1 in Eq. (8) to zero. Fig. 5a and b shows the evolution of transmission rates in the NH and SH countries. From May to September 2020, the non-seasonality transmission rate (blue curve) in NH is generally higher than the transmission rate with seasonality (red curve), while in the SH the transmission rate with seasonality is higher. In other words, the summer season exerts a reducing effect on the transmission rate, while the winter season can enhance the transmission rate. The seasonal variation of transmission rates derived from the modified SEIR model is generally consistent with the seasonal signals extracted by the EEMD method (see Figs. 3 and 4). Studies have found that the survival time of coronavirus on surfaces could depend on the decrease or increase in environmental temperatures (Tan, 2005), and the lower temperature is associated with increasing daily incidence rate. In NH, the temperature usually peaks in July and falls to the lowest in January, whereas in the SH the situation is the opposite. The transmissibility of influenza and several types of coronaviruses may enhance in the SH winter and reduce in the NH summer. Generally, the simulations of both hemispheres and the seasonal signals decomposed by the

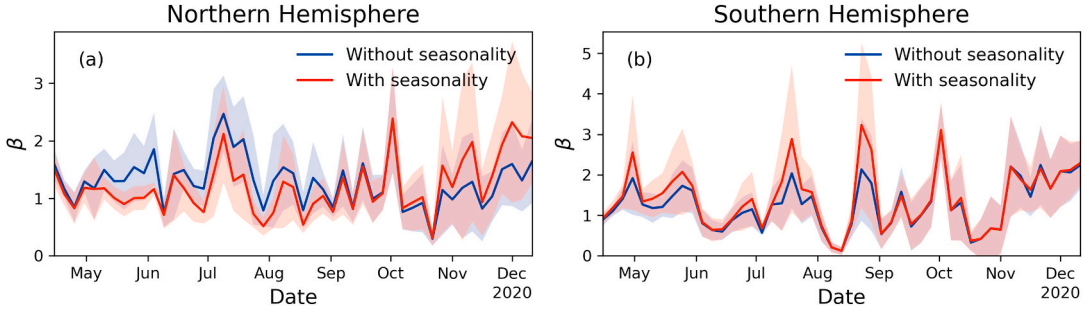

Fig. 5. The average transmission rates (β) in the NH (a) and SH (b) countries, respectively. The red curves show the simulated transmission rate with actual pandemic data (with seasonality), while the blue curves show the transmission rate with seasonality influence excluded (without seasonality). The 90% confidence intervals are indicated by the corresponding color shading.

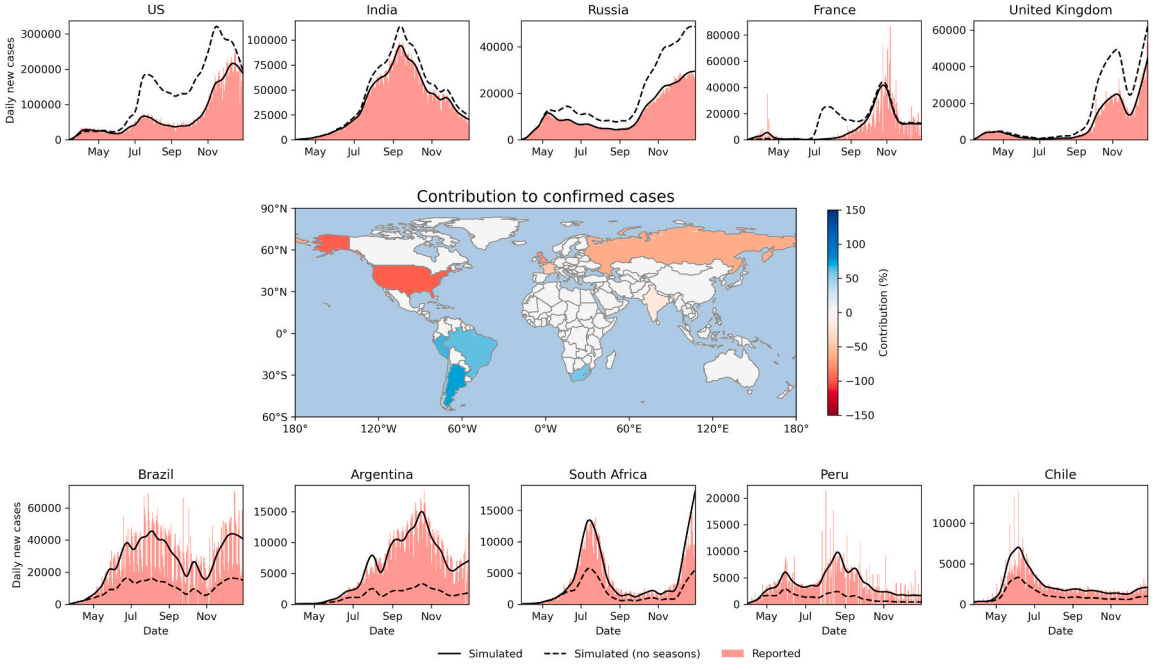

Fig. 6. Daily new cases of COVID-19 in 10 countries. The upper panels show the 5 NH countries, and the lower panels show the 5 SH countries. The red bars denote the reported daily new cases. The solid black curves refer to the simulated daily new cases, and the dotted black curves refer to the simulation with seasonality influence excluded. The contribution of seasonality to the total infections are plotted on the map.

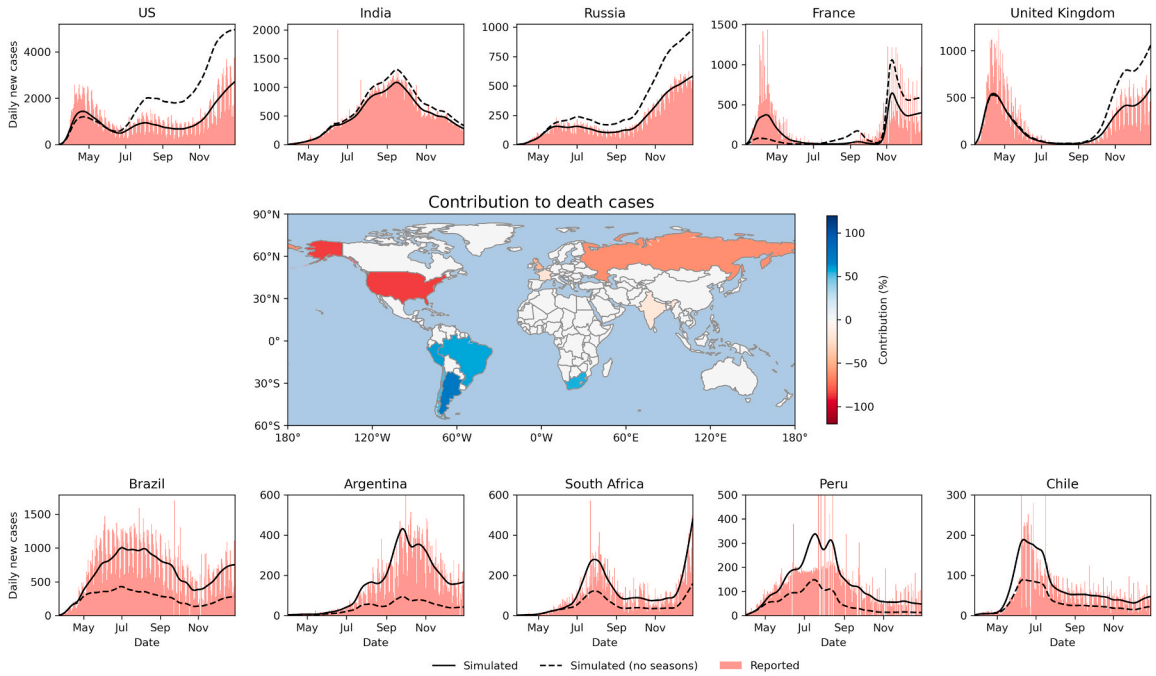

Fig. 7. Same as Fig. 6, but for death cases.

EEMD method corroborate the effect of the seasonal cycle on the transmission rate: the reduction effect in the warm seasons and the amplification effect in the cold seasons.

To explore the contribution of seasonality to the COVID-19 pandemic, we design a scenario that excludes the seasonality factor. In this scenario, the parameters (α, β_0, γ, λ, δ, and κ) remains consistent with the previous simulation, while the seasonality term with β_1 in Eq. (9) is removed to obtain the non-seasonality transmission rate. Figs. 6 and 7 show the simulations of daily increment of confirmed and death cases in the 10 countries, and the contribution of seasonality of each country is mapped. In the NH countries, the number of confirmed and death cases in seasonality scenario is significantly lower compared with the non-seasonality scenario, while in the SH countries the COVID-19 cases in the non-seasonality scenario are significantly higher. The difference between seasonality and non-seasonality scenarios mainly occurs in summer/winter, when changes of environmental conditions are most obvious in an annual cycle. In the SH countries, the total infections in the non-seasonality scenario are 59.71 $\pm$ 8.72% less than the actual total infections, while the non-seasonality scenario can contribute to 46.38 $\pm$ 29.10% of the total infections in the NH countries. However, these results should be interpreted with caution. Since intervention measures in the simulation of the non-seasonality scenario are consistent with the actual situation, the reduction or increment of COVID-19 prevalence in non-seasonality is attributable to the combined effects of non-pharmacological interventions and environmental conditions.

Although seasonal variability may have played an important role in the evolution of the outbreaks, its actual effect is limited. In the simulations of the non-seasonality scenario, none of the outbreaks is completely restrained in the SH countries, and actual pandemic data in the NH reveals no significant downward trend during the summer months. During the first wave of the H1N1 pandemic in 2009, the growth of incidence in NH was still obvious in August, when environmental condition is most unfavorable in the year. At the beginning of an outbreak, the transmission is unlikely to stop even with strong seasonal drivers, because immunity is lacking and almost all the population is susceptible to the disease (Carlson et al., 2020). High susceptibility is a core driver in the early stage of the outbreak (Baker et al., 2020). Therefore, the trajectory of the epidemic depends on a combination of factors, and seasonal variability is insufficient to stop virus transmission. Favorable climate conditions will not be able to reduce the transmissibility of the virus to an extent that interventions are no longer needed to curb its spread.

In addition, the simulations indicate discrepancies in the contribution of seasonality to different regions. In NH countries, the seasonality produces a disincentive effect on COVID-19 development, indicating the reduction caused by the warmer climate, while the seasonality encourages the growth in SH countries. We mapped the distribution of their contribution and found that the contribution of the seasonal cycle is more obvious in high latitude countries, where the local seasonal cycle is more pronounced. We further calculated the standard deviation of the seasonal signals extracted by the EEMD method to quantify the amplitude of seasonal signals, and analyzed their correlation with latitude. The contribution in NH countries derived from the models are all negative, and the seasonal signals in NH and SH countries extracted by the EEMD method are opposite. Therefore, for NH countries, the standard deviations are set to their opposite numbers for the convenience of comparison. Since the COVID-19 cases are reported on country level, a representative latitude for each country should be identified, and factors like the distribution of the human population, economic development, etc. should be taken into account. Here, we use weighted geographic centers derived by global nighttime lights data (Hall et al., 2019) as the representative geographic points (see the red points in Fig. S15). Fig. 8a and b shows the correlation between latitude and the strength of seasonal signals. The EEMD method (qualitative approach) and epidemical model (quantitative approach) corroborate each other, and arrive at an agreement that the seasonal signals are stronger in high latitude countries.

The amplitude of seasonal changes during a year depends strongly on the latitude. For instance, there are only small seasonal changes in temperature at lower latitudes with increasingly larger seasonal changes in temperature at higher latitudes (see Fig. S15a). We further analyze the seasonal amplitude of two meteorological factors (near surface temperature and near surface humidity) and two air quality indicators (total column NO_2 and $PM_{2.5}$ concentrations). Fig. S15 shows the global distribution of the seasonal amplitude of the four environmental indicators. The amplitude of the temperature seasonal cycle is most obvious in high latitude regions, which is directly associated with periodic shifts of subsolar point. Stronger temperature amplitude is observed on land due

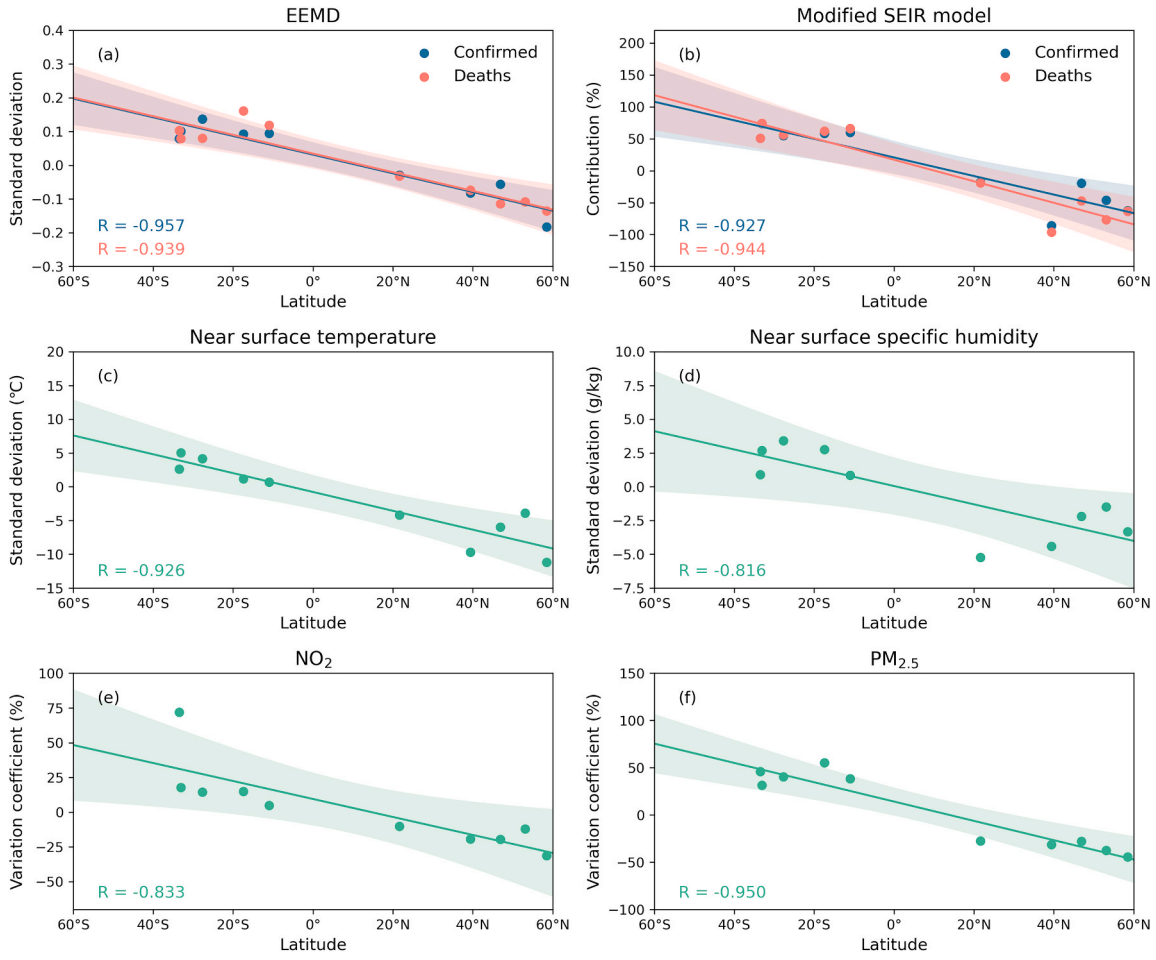

Fig. 8. The correlation between latitude and seasonal signals of COVID-19 pandemic. (a): the amplitude of seasonal signals decomposed by the EEMD method. The amplitude is quantified by the standard deviation of EEMD signals. (b): the contribution of seasonal factors derived from the modified SEIR epidemiological models. The blue dots denote the confirmed cases and red dots denote death cases in (a) and (b). (c ~ f): seasonal amplitude of meteorological (near surface temperature and specific humidity) and environmental factors (total column NO_2 and $PM_{2.5}$ concentrations). The amplitude of the meteorological variable is quantified by the standard deviation of monthly values in an annual cycle, and the amplitude of the air quality indicator is quantified by the coefficient of variation. For the convenience of comparison, the seasonal amplitudes of NH countries are all set to their opposite number.

to the smaller specific heat capacity of land than seawater. For specific humidity, large amplitude is mainly distributed in the monsoon regions, where significant seasonal changes in atmospheric circulation and precipitation associated with the asymmetric heating of land and sea occur. For air quality indicators, large standard deviation is expected in heavily polluted regions, while in the natural background with little or no human activities, the standard deviation is extremely small. Therefore, to make comparison between the dispersion level of data (seasonal amplitude) whose scales of measurement are not comparable, coefficient of variation (the ratio of the standard deviation to the mean) is calculated on each grid to reveal the spatially comparable amplitude. The relationship between the seasonal amplitude of environmental factors and latitudes are shown in Figs. 8 (c ~ f), with larger amplitudes in higher latitudes. Thus, regions with stronger COVID-19 seasonal signals coincide with the regions with stronger environmental seasonal signals. This implies that the COVID-19 pandemic is prone to the influence by the variation of environmental conditions, and the degree of its influence is highly correlated with the amplitude of local environmental conditions. Seasonality is more pronounced at higher latitudes, which may exert a larger impact on the spread of SARS-CoV-2.

3.3. How does seasonality influence the COVID-19 transmission: a set of possible mechanisms

Numerous mechanisms, through which environmental conditions influence the transmission of respiratory viral infections other than COVID-19, have been proposed. Here, based on our qualitative and quantitative assessment of seasonality in COVID-19 transmission, we propose a set of mechanisms on how seasonality can affect the spread of COVID-19 (see Fig. 9). First, variations of environmental conditions due to the seasonal cycle can affect the viability of the virus. Aerosol transmission is identified as one of the potential transmission routes of SARS-CoV-2 (Yao et al., 2020a; Zhang et al., 2020a) and can be enhanced in low humidity environments. Low humidity can induce evaporation of water vapor from the exhaled bioaerosols, contributing to the formation of droplet nuclei that stay suspended in the air for prolonged periods (Tellier, 2006). It has been speculated that cool and dry conditions are especially suitable for aerosol transmission of viruses in temperate winter (Lowen et al., 2008). On the other hand, high humidity would increase the efficiency of contact transmission. High humidity can promote the survival of the virus by influencing the evaporation of virus-containing droplets (Yang et al., 2012). This will influence the survival of the virus on surfaces contaminated by respiratory secretions.

Second, the seasonal cycle of environmental conditions would also

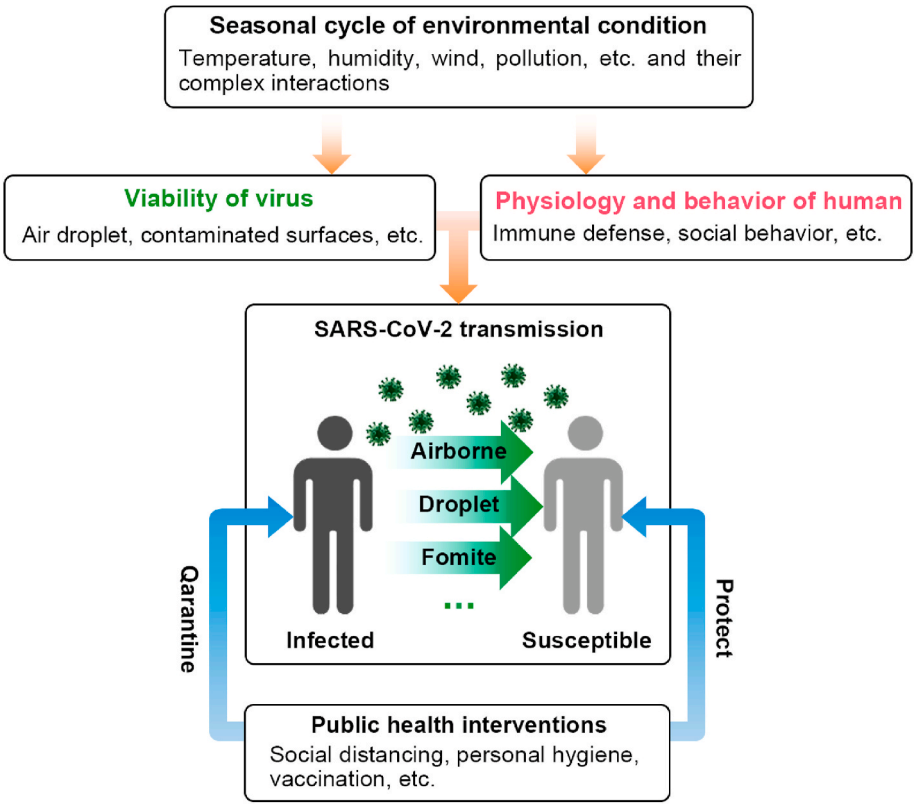

Fig. 9. The role of seasonality in the spread of COVID-19 pandemic.

influence human behaviors and immunity. During the cold and rainy days, people tend to gather and stay indoors, which would exacerbate the risk of infection (Orenes-Piñero et al., 2021). Available contact tracing data indicate a high proportion of indoor infection of SARS-CoV-2 (Qian et al., 2020). Extreme warm weather might also contribute to the spread of the virus. Mask wearing can induce increased facial skin temperature and discomfort, which could lower the wearing adherence in hot and humid weather (Scarano et al., 2020). The use of air conditioners could increase in hot weather, which may also increase the risk of indoor infection (Lu et al., 2020). Additionally, many studies indicated that immune function can be suppressed in cold environments, which would increase the risk of getting infected (Shephard and Shek, 1998). Gathering activities and immunosuppressive effects induced by environmental changes would lead to the accelerated diffusion of COVID-19 and amplify the contribution of seasonality. Studies have also shown that atmospheric pollution may favor coronavirus spreading (Azuma et al., 2020; Fattorini and Regoli, 2020; Zhang et al., 2020b). Analysis of the SARS-CoV-1 and preliminary investigations of SARS-CoV-2 provide evidence that the incidence and severity are related to ambient air pollution (Pozzer et al., 2020). Changes in the sources of air pollution and meteorological factors can result in changes in characteristics of the air pollution mixture across different seasons (Ming et al., 2017; Peng et al., 2005). This will also lead to varying degrees of their health impact in different seasons (Han et al., 2020).

It should be noted, however, that the seasonal cycle can also be manifested in the complex interactions between some sets of environmental and socio-economic variables. For example, air pollution has been proved as an important cofactor on increasing the risk of mortality from COVID-19 (Coccia, 2020b; Pozzer et al., 2020). Air pollution events do not always independently influence the COVID-19, but their combined effects with the meteorological condition can aggravate the health consequence. High-pressure systems, which prevail over landmasses during winter, can create stagnant air. Low wind speeds reduce the dispersion of atmospheric pollutants, which can act as carrier of the SARS-CoV-2 in the air to sustain the diffusion of COVID-19 in the environment (Coccia, 2020a). In summer, low-pressure systems bring wet and windy conditions, which transport local pollutants to a new area and produce clear skies. In the selected 10 countries, $PM_{2.5}$ and NO_2 concentrations are almost all higher during the winter season (see Figs. S18 and 19), which is associated with the seasonal cycle of meteorological factors, including temperature, humidity (see Fig. S16–17), and wind. In addition, since the outbreak, strict social distancing measures have been taken to curb the spread of virus. During the lockdown period, the intensity of human activities has significantly reduced, which leads to improved air quality, and lower COVID-19 infections (Lian et al., 2020b). The improved air quality is a consequence of intense non-pharmacological interventions, and might also potentially contribute to slowing down the COVID-19 transmission along with the lockdown measures. Their complex interactions may also exhibit some form of seasonality to influence the spread of COVID-19 and other diseases. However, the relative contributions of these indicators to the modulation of COVID-19 seasonality warrant further investigations.

4. Conclusions

The COVID-19 pandemic marks the third global outbreak due to a coronavirus after severe acute respiratory syndrome (SARS) in 2003 and the Middle East respiratory syndrome (MERS) in 2012 (Sachs et al., 2020), but MERS and SARS have never spread widely or rapidly enough to show seasonality. SARS-CoV-2 has infected over 100 million people at the time of writing these lines, and it is crucial to understand and project the transmission pattern of COVID-19. Numerical simulations based on the epidemiological model can provide valuable clues on its possible circulating season and how seasonality can influence the patterns of COVID-19 outbreaks.

This study qualitatively and quantitatively analyzes the role of seasonality in the spread of COVID-19. We find that COVID-19 infectivity and mortality of SARS-CoV-2 are both stronger in colder climates, and

COVID-19 seasonality is more pronounced at higher latitudes. Numerical simulation indicates that seasonality alone is not sufficient to stop the virus transmission in the warm season, but it should be taken into account in the future planning of intervention measures. Our findings have important implications in the control and prevention of COVID-19. Rational policy planning aggregated with beneficial effects of seasonal variation may provide a window of opportunity to expand healthcare capacities and develop effective and safe pharmacological treatments. In winter months, cases of COVID-19 may surge along with other coronaviruses' infections and seasonal influenza, which would trigger a substantial increase in the demand for healthcare system resources. Although vaccines have streamed into communities to protect people against coronavirus, scientists warn that herd immunity to the COVID-19 is not likely to be achieved in 2021 (VOA News, 2021).

Nevertheless, our findings are interpreted in the context of several limitations in the study. First, as has been mentioned in Section 2, the seasonality incorporated in the modified SEIR model is an empirical formula [Eq. (9)], which is not undisputed. Here we provide a general framework on how to introduce seasonality into epidemiological models. The equation could be replaced with other functions obtained in future epidemiological and laboratory studies concerning the environmental sensitivities of SARS-CoV-2. By introducing locally specific seasonality function into our model, quantification with greater reliability is anticipated. The model could also be further generalized to quantify the seasonality influence on other infectious diseases and emergent pandemic. In addition, limited public health resources, discrepancies in reporting protocols may have resulted in potential biases in the COVID-19 dataset and added uncertainty to our study. Future research needs to adopt a more comprehensive epidemiological model in conjunction with multisource epidemiological and climate data to quantify the impact of seasonal factors on the spread of COVID-19. The modified SEIR model proposed in this paper is limited to the data on a national or regional scale, and could not be applied to the field data collected from individuals. Based on the results of the epidemiological survey with a special focus on the environmental condition when transmission occurred, we are able to make a broader and clearer assessment of the seasonal patterns of COVID-19 and the underlying mechanisms. However, collecting the field data through the epidemiological survey is a mounting task, considering the meager medical and human resource to undertake extensive survey that is statistically significant when the health system is overloaded. Thus, we suggest that epidemiological survey should be taken in regions where the COVID-19 outbreak is brought under control. Sporadic cases of COVID-19 makes it easier to conduct epidemiological survey with special focus on the environmental conditions when the transmission occurs. Effective multi-discipline collaboration (among epidemiology, environmental science, meteorology, sociology, etc.) is required to illuminate the mechanisms of COVID-19 seasonality.

CRediT author statement

Xiaoyue Liu: Software, Formal analysis, Data curation, Writing - original draft, Writing - review & editing. Jianping Huang: Conceptualization, Supervision, Writing - Review & Editing. Changyu Li: Validation, Writing - review & editing. Yingjie Zhao: Writing- Reviewing and Editing. Danfeng Wang: Writing- Reviewing and Editing. Zhongwei Huang: Supervision, Conceptualization. Kehu Yang: Writing - review & editing.

Declaration of competing interest

The authors declare that they have no known competing financial interests or personal relationships that could have appeared to influence the work reported in this paper.

Acknowledgments

This work was jointly supported by the National Natural Science Foundation of China (41521004) and the Gansu Provincial Special Fund Project for Guiding Scientific and Technological Innovation and Development (2019ZX-06). The authors acknowledge the Center for Systems Science and Engineering at Johns Hopkins University for providing the COVID-19 data. The authors also acknowledge the NOAA/OAR/ESRL PSL, Boulder, Colorado, USA for providing the NCEP Reanalysis Derived data (https://psl.noaa.gov/).

Appendix A. Supplementary data

Supplementary data to this article can be found online at https://doi.org/10.1016/j.envres.2021.110874.

References

Altamimi, A., Ahmed, A.E., 2020. Climate factors and incidence of Middle East respiratory syndrome coronavirus. J. Infect. Public Health 13, 704–708. https://doi.org/10.1016/j.jiph.2019.11.011.

Audi, A., AlIbrahim, M., Kaddoura, M., Hijazi, G., Yassine, H.M., Zaraket, H., 2020. Seasonality of respiratory viral infections: will COVID-19 follow suit? Front. Public Heal. 8 https://doi.org/10.3389/fpubh.2020.567184 annurev-virology-012420-022445.

Azuma, K., Kagi, N., Kim, H., Hayashi, M., 2020. Impact of climate and ambient air pollution on the epidemic growth during COVID-19 outbreak in Japan. Environ. Res. 190, 110042. https://doi.org/10.1016/j.envres.2020.110042.

Baker, R.E., Yang, W., Vecchi, G.A., Metcalf, C.J.E., Grenfell, B.T., 2020. Susceptible supply limits the role of climate in the early SARS-CoV-2 pandemic. Science 369, 315–319. https://doi.org/10.1126/science.abc2535, 80.

Bilal, Bashir M.F., Benghoul, M., Numan, U., Shakoor, A., Komal, B., Bashir, M.A., Bashir, M., Tan, D., 2020. Environmental pollution and COVID-19 outbreak: insights from Germany. Air Qual. Atmos. Health. https://doi.org/10.1007/s11869-020-00893-9.

Cai, Q.-C., Lu, J., Xu, Q.-F., Guo, Q., Xu, D.-Z., Sun, Q.-W., Yang, H., Zhao, G.-M., Jiang, Q.-W., 2007. Influence of meteorological factors and air pollution on the outbreak of severe acute respiratory syndrome. Publ. Health 121, 258–265. https://doi.org/10.1016/j.puhe.2006.09.023.

Cai, W., Li, K., Liao, H., Wang, H., Wu, L., 2017. Weather conditions conducive to Beijing severe haze more frequent under climate change. Nat. Clim. Change 7, 257–262. https://doi.org/10.1038/nclimate3249.

Carlson, C.J., Gomez, A.C.R.R., Bansal, S., Ryan, S.J., 2020. Misconceptions about weather and seasonality must not misguide COVID-19 response. Nat. Commun. 11, 4312. https://doi.org/10.1038/s41467-020-18150-z.

Cheynet, E., 2020. Generalized SEIR Epidemic Model (fitting and computation). Github. [WWW Document] https://github.com/ECheynet/SEIR/releases/tag/v4.8.4.

Chin, A.W.H., Chu, J.T.S., Perera, M.R.A., Hui, K.P.Y., Yen, H.-L., Chan, M.C.W., Peiris, M., Poon, L.L.M., 2020. Stability of SARS-CoV-2 in different environmental conditions. The Lancet Microbe 1, e10. https://doi.org/10.1016/S2666-5247(20)30003-3.

Chowdhury, R., Luhar, S., Khan, N., Choudhury, S.R., Matin, I., Franco, O.H., Reza, S., Imran, C., Oscar, M., 2020. Long-term strategies to control COVID-19 in low and middle-income countries: an options overview of community-based, non-pharmacological interventions. Eur. J. Epidemiol. 1–6. https://doi.org/10.1007/s10654-020-00660-1.

Coccia, M., 2020a. The effects of atmospheric stability with low wind speed and of air pollution on the accelerated transmission dynamics of COVID-19. Int. J. Environ. Stud. 1–27. https://doi.org/10.1080/00207233.2020.1802937, 00.

Coccia, M., 2020b. How do low wind speeds and high levels of air pollution support the spread of COVID-19? Atmos. Pollut. Res. https://doi.org/10.1016/j.apr.2020.10.002.

Coccia, M., 2020c. Factors determining the diffusion of COVID-19 and suggested strategy to prevent future accelerated viral infectivity similar to COVID. Sci. Total Environ. 729, 138474. https://doi.org/10.1016/j.scitotenv.2020.138474.

Coccia, M., 2020d. An index to quantify environmental risk of exposure to future epidemics of the COVID-19 and similar viral agents: theory and practice. Environ. Res. 191, 110155. https://doi.org/10.1016/j.envres.2020.110155.

Colominas, M.A., Schlotthauer, G., Torres, M.E., 2014. Improved complete ensemble EMD: a suitable tool for biomedical signal processing. Biomed. Signal Process Contr. 14, 19–29. https://doi.org/10.1016/j.bspc.2014.06.009.

Coşkun, H., Yıldırım, N., Gündüz, S., 2021. The spread of COVID-19 virus through population density and wind in Turkey cities. Sci. Total Environ. 751, 141663. https://doi.org/10.1016/j.scitotenv.2020.141663.

Davies, N.G., Kucharski, A.J., Eggo, R.M., Gimma, A., Edmunds, W.J., Jombart, T., O'Reilly, K., Endo, A., Hellewell, J., Nightingale, E.S., Quilty, B.J., Jarvis, C.I., Russell, T.W., Klepac, P., Bosse, N.I., Funk, S., Abbott, S., Medley, G.F., Gibbs, H., Pearson, C.A.B., Flasche, S., Jit, M., Clifford, S., Prem, K., Diamond, C., Emery, J., Deol, A.K., Procter, S.R., van Zandvoort, K., Sun, Y.F., Munday, J.D., Rosello, A., Auzenbergs, M., Knight, G., Houben, R.M.G.J., Liu, Y., 2020. Effects of non-pharmaceutical interventions on COVID-19 cases, deaths, and demand for hospital

services in the UK: a modelling study. Lancet Public Health 11–15. https://doi.org/10.1016/S2468-2667(20)30133-X.
Dehning, J., Zierenberg, J., Spitzner, F.P., Wibral, M., Neto, J.P., Wilczek, M., Priesemann, V., 2020. Inferring change points in the spread of COVID-19 reveals the effectiveness of interventions. Science 369, eabb9789. https://doi.org/10.1126/science.abb9789, 80.
Dong, E., Du, H., Gardner, L., 2020. An interactive web-based dashboard to track COVID-19 in real time. Lancet Infect. Dis. 20, 533–534. https://doi.org/10.1016/S1473-3099(20)30120-1.
Fattorini, D., Regoli, F., 2020. Role of the chronic air pollution levels in the Covid-19 outbreak risk in Italy. Environ. Pollut. 264, 114732. https://doi.org/10.1016/j.envpol.2020.114732.
Feng, Y., Marchal, T., Sperry, T., Yi, H., 2020. Influence of wind and relative humidity on the social distancing effectiveness to prevent COVID-19 airborne transmission: a numerical study. J. Aerosol Sci. https://doi.org/10.1016/j.jaerosci.2020.105585.
Glencross, D.A., Ho, T.-R., Camiña, N., Hawrylowicz, C.M., Pfeffer, P.E., 2020. Air pollution and its effects on the immune system. Free Radic. Biol. Med. 151, 56–68. https://doi.org/10.1016/j.freeradbiomed.2020.01.179.
Hall, O., Bustos, M.F.A., Olén, N.B., Niedomysl, T., 2019. Population centroids of the world administrative units from nighttime lights 1992-2013. Sci. Data. https://doi.org/10.1038/s41597-019-0250-z.
Han, L., Sun, Z., He, J., Hao, Y., Tang, Q., Zhang, X., Zheng, C., Miao, S., 2020. Seasonal variation in health impacts associated with visibility in Beijing, China. Sci. Total Environ. 730, 139149. https://doi.org/10.1016/j.scitotenv.2020.139149.
Harko, T., Lobo, F.S.N., Mak, M.K., 2014. Exact analytical solutions of the Susceptible-Infected-Recovered (SIR) epidemic model and of the SIR model with equal death and birth rates. Appl. Math. Comput. 236, 184–194. https://doi.org/10.1016/j.amc.2014.03.030.
Huang, J., Zhang, L., Liu, Xiaoyue, Wei, Y., Liu, C., Lian, X., Huang, Z., Chou, J., Liu, Xingrong, Li, X., Yang, K., Wang, J., Liang, H., Gu, Q., Du, P., Zhang, T., 2020c. Global prediction system for COVID-19 pandemic. Sci. Bull. https://doi.org/10.1016/j.scib.2020.08.002.
Huang, N.E., Wu, Z., 2008. A review on Hilbert-Huang transform: method and its applications to geophysical studies. Rev. Geophys. 46, RG2006. https://doi.org/10.1029/2007RG000228.
Huang, S., Wu, L., Xu, L., Zhang, A., Sheng, L., Liu, F., Zhou, L., Li, J., Hao, R., Qian, H., Fang, S., Li, Yingru, Li, Yuguo, Lu, C., Deng, Q., 2020a. Transmission Dynamics of Coronavirus Disease 2019 (COVID-19) in the World : the Roles of Intervention and Seasonality 2019, pp. 1–43.
Huang, Z., Huang, J., Gu, Q., Du, P., Liang, H., Dong, Q., 2020b. Optimal temperature zone for the dispersal of COVID-19. Sci. Total Environ. 736, 139487. https://doi.org/10.1016/j.scitotenv.2020.139487.
Ji, F., Wu, Z., Huang, J., Chassignet, E.P., 2014. Evolution of land surface air temperature trend. Nat. Clim. Change 4, 462–466. https://doi.org/10.1038/nclimate2223.
Kalnay, E., Kanamitsu, M., Kistler, R., Collins, W., Deaven, D., Gandin, L., Iredell, M., Saha, S., White, G., Woollen, J., Zhu, Y., Leetmaa, A., Reynolds, R., Chelliah, M., Ebisuzaki, W., Higgins, W., Janowiak, J., Mo, K.C., Ropelewski, C., Wang, J., Jenne, R., Joseph, D., 1996. The NCEP/NCAR 40-year reanalysis project. Bull. Am. Meteorol. Soc. 77, 437–471. https://doi.org/10.1175/1520-0477(1996)077<0437:TNYRP>2.0.CO;2.
Kissler, S.M., Tedijanto, C., Goldstein, E., Grad, Y.H., Lipsitch, M., 2020. Projecting the transmission dynamics of SARS-CoV-2 through the postpandemic period. Science 368, 860–868. https://doi.org/10.1126/science.abb5793.
Kraemer, M.U.G., Yang, C.-H., Gutierrez, B., Wu, C.-H., Klein, B., Pigott, D.M., du Plessis, L., Faria, N.R., Li, R., Hanage, W.P., Brownstein, J.S., Layan, M., Vespignani, A., Tian, H., Dye, C., Pybus, O.G., Scarpino, S.V., 2020. The effect of human mobility and control measures on the COVID-19 epidemic in China. Science 368, 493–497. https://doi.org/10.1126/science.abb4218, 80.
Lai, S., Ruktanonchai, N.W., Zhou, L., Prosper, O., Luo, W., Floyd, J.R., Wesolowski, A., Santillana, M., Zhang, C., Du, X., Yu, H., Tatem, A.J., Davies, N.G., Kucharski, A.J., Eggo, R.M., Gimma, A., Edmunds, W.J., Jombart, T., O'Reilly, K., Endo, A., Hellewell, J., Nightingale, E.S., Quilty, B.J., Jarvis, C.I., Russell, T.W., Klepac, P., Bosse, N.I., Funk, S., Abbott, S., Medley, G.F., Gibbs, H., Pearson, C.A.B., Flasche, S., Jit, M., Clifford, S., Prem, K., Diamond, C., Emery, J., Deol, A.K., Procter, S.R., van Zandvoort, K., Sun, Y.F., Munday, J.D., Rosello, A., Auzenbergs, M., Knight, G., Houben, R.M.G.J., Liu, Y., Lai, S., Ruktanonchai, N.W., Zhou, L., Prosper, O., Luo, W., Floyd, J.R., Wesolowski, A., Santillana, M., Zhang, C., Du, X., Yu, H., Tatem, A.J., 2020. Effect of non-pharmaceutical interventions to contain COVID-19 in China. Nature 11–15. https://doi.org/10.1038/s41586-020-2293-x.
Li, Y., Wang, X., Nair, H., 2020a. Global seasonality of human seasonal coronaviruses: a clue for postpandemic circulating season of severe acute respiratory syndrome coronavirus 2? J. Infect. Dis. 222, 1090–1097. https://doi.org/10.1093/infdis/jiaa436.
Laszuk, D., 2017. Python implementation of Empirical Mode Decomposition algorithm. GitHub. https://github.com/laszukdawid/PyEMD. GitHub Repository.
Li, Z., Chen, Q., Feng, L., Rodewald, L., Xia, Y., Yu, H., Zhang, R., An, Z., Yin, W., Chen, W., Qin, Y., Peng, Z., Zhang, T., Ni, D., Cui, J., Wang, Q., Yang, X., Zhang, M., Ren, X., Wu, D., Sun, X., Li, Y., Zhou, L., Qi, X., Song, T., Gao, G.F., Feng, Z., Li, Z., Chen, Q., Feng, L., Rodewald, L., Xia, Y., Yu, H., Zhang, R., Yin, W., Ni, D., Qin, Y., Zhang, T., Cui, J., Wang, Q., Yang, X., Zhang, M., Chen, W., Peng, Z., Ren, X., An, Z., Wu, D., Sun, X., Li, Y., Zhou, L., Qi, X., Gao, G.F., Feng, Z., Song, T., Luo, H., Yin, Z., Wang, L., Ma, C., Li, S., 2020b. Active case finding with case management: the key to tackling the COVID-19 pandemic. Lancet 396, 63–70. https://doi.org/10.1016/S0140-6736(20)31278-2.
Lian, X., Huang, J., Huang, R., Liu, C., Wang, L., Zhang, T., 2020a. Impact of city lockdown on the air quality of COVID-19-hit of Wuhan city. Sci. Total Environ. 742, 140556. https://doi.org/10.1016/j.scitotenv.2020.140556.
Lian, X., Huang, J., Zhang, L., Liu, C., Liu, X., Wang, L., 2020b. Environmental indicator for COVID-19 non-pharmaceutical interventions. Geophys. Res. Lett. https://doi.org/10.1029/2020GL090344.
Lowen, A.C., Steel, J., Mubareka, S., Palese, P., 2008. High temperature (30°C) blocks aerosol but not contact transmission of influenza virus. J. Virol. 82, 5650–5652. https://doi.org/10.1128/JVI.00325-08.
Lu, J., Gu, J., Gu, J., Li, K., Xu, C., Su, W., Lai, Z., Zhou, D., Yu, C., Xu, B., Yang, Z., 2020. COVID-19 outbreak associated with air conditioning in restaurant, Guangzhou, China, 2020. Emerg. Infect. Dis. https://doi.org/10.3201/eid2607.200764.
Ma, J., Qi, X., Chen, H., Li, X., Zhang, Z., Wang, H., Sun, L., Zhang, L., Guo, J., Morawska, L., Grinshpun, S.A., Biswas, P., Flagan, R.C., Yao, M., 2020. Coronavirus disease 2019 patients in earlier stages exhaled millions of severe acute respiratory syndrome coronavirus 2 per hour. Clin. Infect. Dis. https://doi.org/10.1093/cid/ciaa1283.
Mahase, E., 2021. Covid-19: what new variants are emerging and how are they being investigated? BMJ n158. https://doi.org/10.1136/bmj.n158.
Martinez, M.E., 2018. The calendar of epidemics: seasonal cycles of infectious diseases. PLoS Pathog. 14, e1007327 https://doi.org/10.1371/journal.ppat.1007327.
Matson, M.J., Yinda, C.K., Seifert, S.N., Bushmaker, T., Fischer, R.J., van Doremalen, N., Lloyd-Smith, J.O., Munster, V.J., 2020. Effect of environmental conditions on SARS-CoV-2 stability in human nasal mucus and sputum. Emerg. Infect. Dis. 26, 2276–2278. https://doi.org/10.3201/eid2609.202267.
Ming, L., Jin, L., Li, J., Fu, P., Yang, W., Liu, D., Zhang, G., Wang, Z., Li, X., 2017. PM2.5 in the Yangtze River Delta, China: chemical compositions, seasonal variations, and regional pollution events. Environ. Pollut. https://doi.org/10.1016/j.envpol.2017.01.013.
Oran, D.P., Topol, E.J., 2020. Prevalence of asymptomatic SARS-CoV-2 infection. Ann. Intern. Med. 19, 19–21. https://doi.org/10.7326/m20-3012.
Orenes-Piñero, E., Baño, F., Navas-Carrillo, D., Moreno-Docón, A., Marín, J.M., Misiego, R., Ramírez, P., 2021. Evidences of SARS-CoV-2 virus air transmission indoors using several untouched surfaces: a pilot study. Sci. Total Environ. 751, 142317. https://doi.org/10.1016/j.scitotenv.2020.142317.
Peng, L., Yang, W., Zhang, D., Zhuge, C., Hong, L., Liangrong, P., Wuyue, Y., Dongyan, Z., Changjing, Z., Liu, H., 2020. Epidemic analysis of COVID-19 in China by dynamical modeling. medRxiv 1–18. https://doi.org/10.1101/2020.02.16.20023465.
Peng, R.D., Dominici, F., Pastor-Barriuso, R., Zeger, S.L., Samet, J.M., 2005. Seasonal analyses of air pollution and mortality in 100 US cities. Am. J. Epidemiol. 161, 585–594. https://doi.org/10.1093/aje/kwi075.
Potvin, L., 2021. Is the end of the pandemic really in sight? Can. J. Public Health. https://doi.org/10.17269/s41997-020-00465-5.
Pozzer, A., Dominici, F., Haines, A., Witt, C., Münzel, T., Lelieveld, J., 2020. Regional and global contributions of air pollution to risk of death from COVID-19. Cardiovasc. Res. 116, 2247–2253. https://doi.org/10.1093/cvr/cvaa288.
Prata, D.N., Rodrigues, W., Bermejo, P.H., 2020. Temperature significantly changes COVID-19 transmission in (sub)tropical cities of Brazil. Sci. Total Environ. 729, 138862. https://doi.org/10.1016/j.scitotenv.2020.138862.
Qian, H., Miao, T., Liu, L., Xiaohong, Z., Luo, D., Li, Y., 2020. Indoor transmission of SARS-CoV-2. medRxiv. https://doi.org/10.1101/2020.04.04.20053058.
Ratnesar-Shumate, S., Williams, G., Green, B., Krause, M., Holland, B., Wood, S., Bohannon, J., Boydston, J., Freeburger, D., Hooper, I., Beck, K., Yeager, J., Altamura, L.A., Biryukov, J., Yolitz, J., Schuit, M., Wahl, V., Hevey, M., Dabisch, P., 2020. Simulated sunlight rapidly inactivates SARS-CoV-2 on surfaces. J. Infect. Dis. https://doi.org/10.1093/infdis/jiaa274.
Rendana, M., 2020. Impact of the wind conditions on COVID-19 pandemic: a new insight for direction of the spread of the virus. Urban Clim. https://doi.org/10.1016/j.uclim.2020.100680.
Sachs, J.D., Horton, R., Bagenal, J., Amor, Y. Ben, Caman, O.K., Lafortune, G., 2020. The lancet COVID-19 commission. Lancet (London, England) 6736, 19–20. https://doi.org/10.1016/S0140-6736(20)31494-X.
Sajadi, M.M., Habibzadeh, P., Vintzileos, A., Shokouhi, S., Miralles-Wilhelm, F., Amoroso, A., 2020. Temperature, humidity, and latitude analysis to estimate potential spread and seasonality of coronavirus disease 2019 (COVID-19). JAMA Netw. Open 3, e2011834. https://doi.org/10.1001/jamanetworkopen.2020.11834.
Scarano, A., Inchingolo, F., Lorusso, F., 2020. Facial skin temperature and discomfort when wearing protective face masks: thermal infrared imaging evaluation and hands moving the mask. Int. J. Environ. Res. Publ. Health 17, 4624. https://doi.org/10.3390/ijerph17134624.
Shephard, R.J., Shek, P.N., 1998. Cold exposure and immune function. Can. J. Physiol. Pharmacol. https://doi.org/10.1139/y98-097.
Tan, J., 2005. An initial investigation of the association between the SARS outbreak and weather: with the view of the environmental temperature and its variation. J. Epidemiol. Community Health 59, 186–192. https://doi.org/10.1136/jech.2004.020180.
Tellier, R., 2006. Review of aerosol transmission of influenza A virus. Emerg. Infect. Dis. 12, 1657–1662. https://doi.org/10.3201/eid1211.060426.
Tong, S., 2019. Air pollution and disease burden. Lancet Planet. Heal. 3, e49–e50. https://doi.org/10.1016/S2542-5196(18)30288-2.
van Doremalen, N., Bushmaker, T., Morris, D.H., Holbrook, M.G., Gamble, A., Williamson, B.N., Tamin, A., Harcourt, J.L., Thornburg, N.J., Gerber, S.I., Lloyd-Smith, J.O., de Wit, E., Munster, V.J., 2020. Aerosol and surface stability of SARS-CoV-2 as compared with SARS-CoV-1. N. Engl. J. Med. 382, 1564–1567. https://doi.org/10.1056/NEJMc2004973.

VOA News, 2021. COVID-19 Herd Immunity Will Not Be Achieved in 2021, WHO Says [WWW Document]. VOA News. accessed 1.15.21. https://www.voanews.com/covid-19-pandemic/covid-19-herd-immunity-will-not-be-achieved-2021-who-says.

WHO, 2021. COVID-19 Weekly Epidemiological Update - 12 January 2021 [WWW Document]. accessed 1.13.21. https://www.who.int/docs/default-source/coronaviruse/situation-reports/weekly_epidemiological_update_22.pdf.

Wilson, N., Corbett, S., Tovey, E., 2020. Airborne transmission of Covid-19. BMJ. https://doi.org/10.1136/bmj.m3206 m3206.

Wu, X., Nethery, R.C., Sabath, M.B., Braun, D., Dominici, F., 2020. Air pollution and COVID-19 mortality in the United States: strengths and limitations of an ecological regression analysis. Sci. Adv. https://doi.org/10.1126/SCIADV.ABD4049.

Wu, Z., Huang, N.E., Long, S.R., Peng, C.K., 2007. On the trend, detrending, and variability of nonlinear and nonstationary time series. Proc. Natl. Acad. Sci. U. S. A. https://doi.org/10.1073/pnas.0701020104.

Xie, J., Zhu, Y., 2020. Association between ambient temperature and COVID-19 infection in 122 cities from China. Sci. Total Environ. 724, 138201. https://doi.org/10.1016/j.scitotenv.2020.138201.

Yanes-Lane, M., Winters, N., Fregonese, F., Bastos, M., Perlman-Arrow, S., Campbell, J. R., Menzies, D., 2020. Proportion of asymptomatic infection among COVID-19 positive persons and their transmission potential: a systematic review and meta-analysis. PloS One 15, e0241536. https://doi.org/10.1371/journal.pone.0241536.

Yang, W., Elankumaran, S., Marr, L.C., 2012. Relationship between humidity and influenza A viability in droplets and implications for influenza's seasonality. PloS One 7, e46789. https://doi.org/10.1371/journal.pone.0046789.

Yao, M., Zhang, L., Ma, J., Zhou, L., 2020a. On airborne transmission and control of SARS-Cov-2. Sci. Total Environ. 731, 139178. https://doi.org/10.1016/j.scitotenv.2020.139178.

Yao, Y., Pan, J., Liu, Z., Meng, X., Wang, Weidong, Kan, H., Wang, Weibing, 2020b. No association of COVID-19 transmission with temperature or UV radiation in Chinese cities. Eur. Respir. J. https://doi.org/10.1183/13993003.00517-2020.

Zhang, R., Li, Y., Zhang, A.L., Wang, Y., Molina, M.J., 2020a. Identifying airborne transmission as the dominant route for the spread of COVID-19. Proc. Natl. Acad. Sci. Unit. States Am. 117, 202009637. https://doi.org/10.1073/pnas.2009637117.

Zhang, Z., Xue, T., Jin, X., 2020b. Effects of meteorological conditions and air pollution on COVID-19 transmission: evidence from 219 Chinese cities. Sci. Total Environ. 741, 140244. https://doi.org/10.1016/j.scitotenv.2020.140244.